Finite element modeling to expand the UMCCA model to describe biofilm mechanical behavior

C.S. Laspidou*,, B.E. Rittmann** and S.A. Karamanos*****

*Department of Civil Engineering, University of Thessaly, Pedion Areos, GR-38334 Volos, Greece (E-mail: *c-laspidou@northwestern.edu*)

**Department of Civil and Environmental Engineering, Northwestern University, 2145 Sheridan Road, Evanston, IL 60208-3109, USA (E-mail: *b-rittmann@northwestern.edu*)

***Department of Mechanical and Industrial Engineering, University of Thessaly, Pedion Areos, GR-38334 Volos, Greece (E-mail: *skara@uth.gr*)

Abstract In order to understand the influence of biofilm's physical and microbiological structures on its mechanical behavior, a finite element model that describes the structural mechanics of a composite solid is linked to the outputs of the multi-component biofilm model UMCCA. The UMCCA model outputs densities of active biomass, inert biomass, and EPS for each compartment in a 2-D biofilm. These densities are mapped to the finite-element model to give a composite Young's modulus, which expresses the stress-strain properties of the biofilm by location. Sample results illustrate that using this methodology, one can identify the points in the biofilm that develop the highest internal stresses and that are most likely to fail first, leading to detachment.

Keywords Biofilm; elasticity; EPS; finite element analysis; numerical modeling

Water Science & Technology **Vol 52 No 7 pp 161–166** © IWA Publishing 2005

Introduction

Whether we want to promote "good" biofilm or eliminate "bad" biofilm, its accumulation depends on the biofilm's mechanical strength, or its ability to sustain forces that scour or abrade the biofilm off the surface. The mechanical behavior of the biofilm depends on the composition and density of the biomass in the biofilm. The common wisdom is that EPS (extracellular polymeric substances) are the bacterially secreted "glue" that binds the active bacteria and inert (or dead) bacteria to each other and the surface. Furthermore, the local densities of EPS and the other components determine mechanical strength at a location in the biofilm.

We developed the Unified Multiple-Component Cellular Automaton (UMCCA) model (Laspidou and Rittmann, 2004a) that describes quantitatively the biofilm's heterogeneity for the key components of a biofilm system: three solid species (active bacteria, inert or biomass, and EPS) and four soluble components (soluble substrate, two types of soluble microbial products (SMP), and oxygen). This model builds on our unified theory, which reconciles the apparently disparate findings about active and inert biomass, EPS, and SMP (Laspidou and Rittmann, 2002a,b). The UMCCA model represents a growing biofilm using a cellular-automaton (CA) approach in which the biofilm grows in a two-dimensional domain of compartments. The UMCCA model also introduces biofilm consolidation, which naturally leads to high biomass density in mature biofilm.

Outputs of the UMCCA model (Laspidou and Rittmann, 2004b) show trends that should bear directly on the mechanical strength of biofilm and its detachment rate. (1) The top of the biofilm is dominated by active biomass and EPS, while the bottoms are dominated by residual inert biomass. (2) The tops of all biofilms are "fluffier" than the bottoms, while the bottoms are more compact. This occurs because biomass in the top rows has not had time to fill in all the space or consolidate to a high density. Some

Downloaded from https://iwaponline.com/wst/article-pdf/52/7/161/434334/161.pdf
by guest

biofilms have finger-like formations with empty spaces between them. (3) All biomass types show considerable local heterogeneity, even with no finger-like formations.

The present work is aimed at describing the influence of biofilm's physical and microbial structures on its deformation under external loads, based on structural mechanics concepts. A finite-element (FE) model of the biofilm is developed with material properties based on the microbial and physical structures generated by the UMCCA model. A general-purpose FE model is employed for the analysis of the biofilm, and a special interface that links the FE program with the UMCCA model is developed. The loading pattern is motivated by the experimental work described by Ohashi *et al.* (1999). Using this modeling technique, two biofilm patterns are analyzed and the results are compared. The results show that our technique can be used for the stress analysis of biofilms and constitutes a first step towards understanding biofilm's strength and resistance to detachment.

Materials and methods

Simulated biofilm samples

The biofilm is represented as an elastic medium in which the material is linearly elastic and isotropic. More specifically, the biofilm is treated as a homogeneous composite material by the methodology of Willis (1980) to estimate the overall properties of the biofilm. The methodology yields a local composite Young's modulus (E_{comp} = the slope of the uniaxial stress–strain curve) based on the relative amounts of the three solid component materials (EPS, active biomass, and inert biomass predicted by the UMCCA model) for each biofilm compartment. Consequently, E_{comp} varies in space according to the spatial variation of the three material components.

Young's modulus values for each solid species are selected from the literature. Although relevant information is scarce, the estimated values of E are reasonable and intuitive. The value of E determines the "stiffness" of the material. In other words, for a given stress (force per unit area), we expect to have the least strain (i.e., deformation per unit length) for residual inert biomass (thus, the highest E), which is relatively rigid. Moreover, Ohashi *et al.* (1999) showed a positive association of the elastic coefficient to total biofilm density; thus, the value of E_{res} (the Young's modulus coefficient associated to the residual dead biomass) is associated to the highest value found in the literature (240 Pa in Stoodley *et al.* (1999)). Since EPS is gelatinous and should deform easily, it has a lower E; thus, the intermediate value of 60 Pa (Picioreanu *et al.*, 2001) is associated to E_{EPS}. The lowest value found in the literature (10 Pa in Stoodley *et al.* (1999)) is associated to the active biomass (E_a), the lowest density species in strong biofilms. Poisson's ratio is assumed equal to 0.3 for all three solid species, as in Picioreanu *et al.* (2001).

Following Willis (1980), the composite E for each compartment is calculated by an approach developed for a composite material that is composed of N isotropic phases with mass ratios c_r, shear moduli μ_r, and bulk moduli κ_r ($r = 1, 2, \ldots N$). In the present case, $N = 3$. The two moduli (shear μ and bulk κ) are related to E and ν (the Poisson ratio) for any solid component by the well-known elasticity formulae:

$$\mu = \frac{E}{2(1+\nu)} \text{ and } \kappa = \frac{\nu \cdot E}{(1+\nu)(1-2\nu)}$$

In each compartment of the composite material, $r - 1$ phases are uniformly and isotropically distributed in the "parent phase." In this work, EPS is the parent phase, since it is the matrix in which other solid species (active and inert biomass) are enveloped.

Downloaded from https://iwaponline.com/wst/article-pdf/52/7/161/434334/161.pdf
by guest

Subsequently, we define the composite shear and bulk modulus as (Willis, 1980):

$$\mu_{comp} = \left\{ \sum_{r=1}^{3} c_r \frac{5\hat{\mu}(3\hat{\kappa} + 4\hat{\mu})}{6\mu_r(\hat{\kappa} + 2\hat{\mu}) + \hat{\mu}(9\hat{\kappa} + 8\hat{\mu})} \right\}^{-1} \sum_{r=1}^{3} c_r \frac{5\hat{\mu}(3\hat{\kappa} + 4\hat{\mu})\mu_r}{6\mu_r(\hat{\kappa} + 2\hat{\mu}) + \hat{\mu}(9\hat{\kappa} + 8\hat{\mu})} \quad (1)$$

$$\kappa_{comp} = \left\{ \sum_{r=1}^{3} c_r \frac{(3\hat{\kappa} + 4\hat{\mu})}{(3\kappa_r + 4\hat{\mu})} \right\}^{-1} \sum_{r=1}^{3} c_r \frac{(3\hat{\kappa} + 4\hat{\mu})\kappa_r}{(3\kappa_r + 4\hat{\mu})} \quad (2)$$

where $\hat{\mu} = \mu_3$ and $\hat{\kappa} = \kappa_3$ are the moduli of the parent phase. Note that Poisson's ratio is equal to 0.3 for all three phases ($v_r = v_{comp} = 0.3$, for $r = 1, 2, 3$). Using the values of μ_{comp} and κ_{comp}, we solve for the composite Young's modulus as: $E_{comp} = 2\mu_{comp}(1 + \nu_{comp})$.

We consider two different biofilm materials to illustrate the numerical methodology. These are outputs generated by UMCCA and are the same simulations shown in Laspidou and Rittmann (2004b) as the "standard case" (Figure 2(a) in Laspidou and Rittmann, 2004b) and "the reduced s_{max} case" (Figure 2(e) in Laspidou and Rittmann, 2004b). They are referred to as "biofilm I" and "biofilm II," respectively. The two biofilms are quite different, as biofilm I is a young biofilm (24.5 days old) and develops in a mat-like formation, while biofilm II is much older (221 days old), is almost completely inert at its bottom, has biofilm densities much higher than biofilm I, and has "mushroom" formations. In Figure 1, the biofilm composite density graphs (repeated from Laspidou and Rittmann (2004b)) and corresponding biofilm composite Young's modulus are presented in a shading format, giving each modeling compartment a shade of gray that is proportional to the density (or E_{comp}): a compartment that is filled 100% (or has the highest E_{comp} value) is colored black, while an empty compartment is white. Corresponding shading scales accompany the plots. UMCCA produces similar plots for all biomass types (not shown in the interest of saving space).

The range of characteristics produced by UMCCA are shown in Figure 1(a) and (d): the biofilm could be relatively flat or "mat-like," or it can have an irregular "mushroom-like" front; adjacent compartments show considerable heterogeneity; the bottom rows are high in density and the top rows contain fluffier (lower density) biofilm. Although biofilm

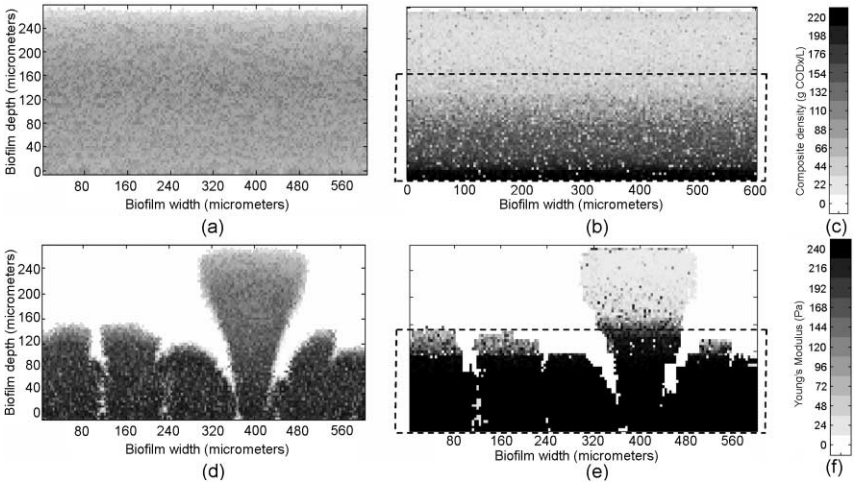

Figure 1 Composite density plots: (a) for biofilm I and (d) for biofilm II, composite Young's modulus (E_{comp}): (b) for biofilm I and (d) for biofilm II. Corresponding shading scales: (c) for composite density and (f) for Young's modulus. Dashed line encloses sections input in ABAQUS

Downloaded from https://iwaponline.com/wst/article-pdf/52/7/161/434334/161.pdf
by guest

composite density and Young's modulus (Figure 1(b) and (e)) correlate in a general way (dark, or light, compartments are dark, or light, in both plots), the correspondence is not exact. The correlation is stronger between E and the density of the inert residual biomass (shading plots not shown), because E_{comp} is a non-linear combination of the effects from each solid component, as shown in equations (1) and (2).

FE modeling

To solve the stress analysis problem of such a non-homogeneous material, we use an FE discretization of the biofilm into solid elements of elastic material. The analysis is performed with the general-purpose finite element program ABAQUS (Hibbit *et al.*, 2003), which has excellent pre-processing and post-processing capabilities, has a large library of finite elements, and has provided excellent results in structural problems regarding the ultimate strength of deformable solids and structures, in comparison with experimental data (Karamanos and Eleftheriadis, 2004).

A special feature of the FE model arises from the high non-homogeneity of the biofilm material. Given the fact that the relative amounts of the three solid species may be quite different in adjacent locations within the biofilm, the elastic properties of the composite biofilm material are unique at each location within the biofilm. This means that the relative amounts of the three solid species are mapped to the FE model from the UMCCA model and used to estimate E_{comp} at all locations in the two-dimensional biofilm. ABAQUS treats this problem as a composite that comprises a large number of different materials, as many as the number of elements (or number of modeling compartments calculated by UMCCA). ABAQUS has a limitation of approximately 3,000 different materials, which in this case means a limitation of 3,000 finite elements or compartments. This is the reason why only a section of the biofilm sample was input in ABAQUS: only the section that was expected to have internal stresses greater than zero. That section is enclosed by a dashed line in Figure 1 (parts (b) and (e)). Also, to reduce the number of elements, the values of E_{comp} for each pair of horizontally adjacent compartments were averaged to one; therefore, the size of each compartment is $4\,\mu m \times 8\,\mu m$ long, as opposed to the $4\,\mu m \times 4\,\mu m$ compartments produced by UMCCA.

For simplicity, each compartment generated by the UMCCA model constitutes one FE of the structural model. Towards this purpose, we developed a special interface between the UMCCA model and the FE program to "communicate" the information between the two models. This interface is an in-house source code and refers to rectangular grids. Extension of this methodology to include non-regular geometries (e.g. curved boundaries) is possible, but it is not considered in the present paper. Therefore, empty spaces that create the irregular biofilm front could not be input in ABAQUS, so they were input as materials with E close to zero.

Results and discussion

Simulated load conditions

The loading pattern is motivated by the work of Ohashi *et al.* (1999), who performed experimental uniaxial testing of biofilm materials. In particular, biofilm was developed around 4.76-mm-diameter adjacent (non-connected) cylinders. Subsequently, the overall mechanical response of the biofilm material was measured as the cylinders were pulled apart. These load conditions are shown schematically in Figure 2(a). For the sake of simplicity, the biofilm material is assumed to be axisymmetric with respect to the cylinder axis. Therefore, no variations of geometry, material properties, or boundary conditions exist in the circumferential cylinder direction (i.e. around the cylinders). Under that assumption, the problem becomes two-dimensional, so that only one slice of biofilm

Downloaded from https://iwaponline.com/wst/article-pdf/52/7/161/434334/161.pdf
by guest

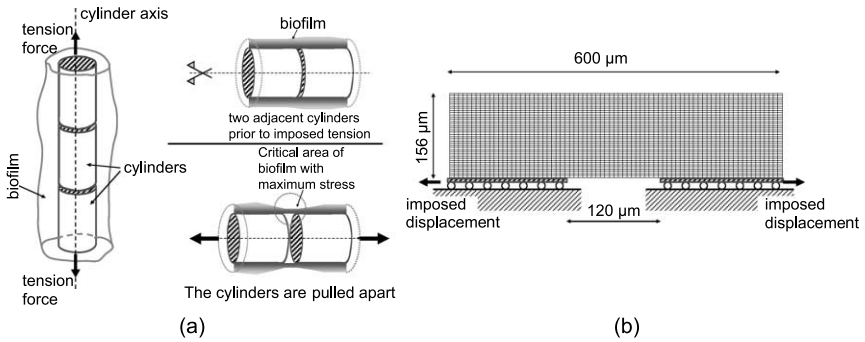

Figure 2 (a) Schematic representation of the loading conditions, motivated by the experiments of Ohashi *et al.* (1999). (b) FE mesh and boundary conditions employed in the present analysis

material is analyzed under axisymmetric conditions. To simulate those conditions, axisymmetric solid elements are employed in the FE discretization. A typical two-dimensional mesh used in the present simulation is shown in Figure 2(b). The biofilm section to be analyzed is within the rectangular grid. The horizontal dimension of the biofilm is 600 μm, whereas its vertical dimension is 156 μm. No sliding between the biofilm and the cylinder is considered. Following this assumption, the "bottom" part of the biofilm is composed of three parts. The left and the right part are connected to rigid boundaries (representing the adjacent left and right cylinders, respectively), whereas the middle part is free and represents the "gap" between the two cylinders. To simulate the experimental procedure, the left and the right parts are subjected to an imposed relative unit displacement. Under this loading pattern, deformations and stresses are computed within the biofilm material.

Figure 3(a, b) shows a sample result from the FE model for the grid shown in Figure 2(b) and for biofilm I depicted in Figure 1(a, b). Figure 3(a) shows the deformed biofilm with its FE mesh, and Figure 3(b) shows the distribution of equivalent (von Mises) stresses within the biofilm material in its deformed configuration. The colors correspond to different stresses in the biofilm. From the distribution of the von Mises stresses and setting a failure criterion, it is possible to determine which parts of the biofilm are most likely to fail first, i.e. where the biofilm is most likely to start developing cracks or to start failing (detachment event). As expected, all of the stresses and deformations (thinning of the biofilm) develop in the critical region of the biofilm, where the cylinders are pulled apart, which is where the samples actually failed for Ohashi *et al.* (1999).

The analysis is repeated for biofilm II. Figure 3(c, d) shows a sample result from the FE model for the grid shown in Figure 2(b), and for biofilm II depicted in Figure 1(d, e).

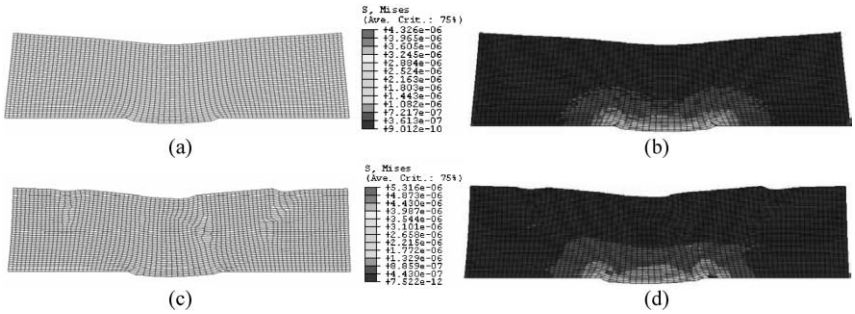

Figure 3 (a) Deformed biofilm I and (c) biofilm II under tensile load conditions, showing FE mesh. (b) Graphical output of von Mises stresses distribution of biofilm I and (d) biofilm II

Downloaded from https://iwaponline.com/wst/article-pdf/52/7/161/434334/161.pdf
by guest

When comparing the two samples, we see that biofilm II has higher E values than biofilm I, and the largest percentage of elements in biofilm II have the highest E_{comp} value of 240 Pa (most of biofilm II is black in Figure 1(e)). This sample shows larger deformations than biofilm I, especially in those areas where there were empty spaces. This occurs because of the low E in those elements, although the stresses remain close to zero there. The von Mises stresses that develop are higher in biofilm II, and this is due to the higher E values throughout this sample. This is obvious when one compares the scale of stresses in Figure 3. From the relationship of stress (σ) and strain (ε) ($\sigma = E \times \varepsilon$) and given that the same deformation (strain) is imposed on the two samples (biofilms I and II), the sample with the higher E (biofilm II) will develop higher stresses. If both materials had the same tensile strength and were subjected to the same deformation, biofilm II would fail first, since the stresses developed in it are higher. However, Ohashi *et al.* (1999) provide experimental data that suggest the argument that biofilm samples with higher E may have higher tensile strength; so this is a fact that needs to be further investigated.

It should be noted that a thorough investigation of biofilm mechanical behavior under various loading conditions through numerical simulation should be based on appropriate experimental data. Nevertheless, such experimental data do not exist. Thus, it is important to develop novel experimental techniques for measuring biofilm structural properties. This constitutes a major challenge, since new techniques are necessary to measure biofilm density, stress, and strain at the micro-scale and in a gel-like medium.

Conclusions

A finite-element model is developed for biofilm stress analysis with material properties based on the results of UMCCA, accounting for biofilm's heterogeneity in terms of its key components. FE results from two biofilm patterns indicate that "stiffer" biofilm regions exhibit higher stresses. Using this FE model an efficient biofilm stress analysis can be conducted, which constitutes a first step towards understanding biofilm's strength and resistance to detachment.

References

Hibbit, H.D., Karlsson, B.I. and Sorensen, P. (2003). Theory Manual, ABAQUS, version 6.3, Providence, RI, USA.

Karamanos, S.A. and Elftheriadis, C. (2004). Collapse of pressurized elastoplastic tubular members under lateral loads. *Int. J. Mech. Sci.*, **46**(1), 35–56.

Laspidou, C.S. and Rittmann, B.E. (2002a). A unified theory for extracellular polymeric substances, soluble microbial products, and active and inert biomass. *Wat. Res.*, **36**, 2711–2720.

Laspidou, C.S. and Rittmann, B.E. (2002b). Non-steady state modeling of extracellular polymeric substances, soluble microbial products, and active and inert biomass. *Wat. Res.*, **36**, 1983–1992.

Laspidou, C.S. and Rittmann, B.E. (2004a). Modeling the development of biofilm density including active bacteria, inert biomass, and extracellular polymeric substances. *Wat. Res.*, **38**(14/15), 3349–3361.

Laspidou, C.S. and Rittmann, B.E. (2004b). Evaluating trends in biofilm density using the UMCCA model. *Wat. Res.*, **38**(14/15), 3362–3372.

Ohashi, A., Koyama, T., Syutsubo, K. and Harada, H. (1999). A novel method for evaluation of biofilm tensile strength resisting to erosion. *Wat. Sci. Tech.*, **39**(7), 261–268.

Picioreanu, C., van Loosdrecht, M.C.M. and Heijnen, J.J. (2001). 2-Dimensional model of biofilm detachment caused by internal stress from liquid flow. *Biotech. Bioeng.*, **72**, 205–218.

Stoodley, P., Lewandowski, Z., Boyle, J.D. and Lappin-Scott, H.M. (1999). Structural deformation of bacterial biofilms caused by short-term fluctuations in fluid shear. *Biotech. Bioeng.*, **65**, 83–92.

Willis, J.R. (1980). Elasticity theory of composites. In *Mechanics of Solids*, Hopkins, H.G. and Sewell, M.J. (eds), Pergamon Press, Oxford.

Downloaded from https://iwaponline.com/wst/article-pdf/52/7/161/434334/161.pdf
by guest